Research Square

Preprints are preliminary reports that have not undergone peer review.
They should not be considered conclusive, used to inform clinical practice,
or referenced by the media as validated information.

Longitudinal evaluation of primary uterine leiomyoma cells reveals culture-dependent shifts in molecular identity and drug responsiveness

NaNa Kang
Keimyung University, School of Medicine
Bok-Ran Choi
Keimyung University, School of Medicine
Hye-Ra Jung
Keimyung University, School of Medicine
Hyowon Hong
Keimyung University, School of Medicine
Chi-Heum Cho
c0035@dsmc.or.kr

Keimyung University, School of Medicine

Article

Keywords: Uterine leiomyoma, Primary cell culture, Longitudinal in vitro analysis, Phenotypic drift, Hormone responsiveness

Posted Date: July 3rd, 2026

DOI: https://doi.org/10.21203/rs.3.rs-9993475/v1

License: This work is licensed under a Creative Commons Attribution 4.0 International License. Read Full License

Additional Declarations: No competing interests reported.

Version of Record: A version of this preprint was published at Scientific Reports on October 6th, 2026. See the published version at https://doi.org/10.1038/s41598-026-69254-3.

Abstract

Uterine leiomyomas (ULs) are typically benign, yet they severely impair female fertility and reproductive health, representing a major unmet clinical need. While primary two-dimensional (2D) culture is widely utilized to study ULs, the longitudinal stability of these cells in standard environments remains poorly characterized. Herein, we systematically evaluated how experimental parameters and serial 2D passaging influence the molecular identity and drug responsiveness of patient-derived UL cells. Morphological, transcriptomic, and functional analyses revealed a rapid culture-induced loss of native tissue identity. Targeted gene profiling demonstrated that estrogen and progesterone receptor mRNA levels dropped precipitously by passage 2, followed by a progressive decline in the smooth muscle marker *ACTA2*. Although optimized media transiently enhanced early hormone responsiveness, it failed to prevent long-term phenotypic drift. Furthermore, drug responses to selective progesterone receptor modulators (SPRMs) were highly context-dependent, significantly altered by prolonged culture and media composition. These results demonstrate that primary UL cells undergo rapid transcriptional reprogramming, leading to unstable pharmacological behavior. Consequently, defining a strictly restricted culture window at early passages establishes an indispensable methodological baseline to prevent artefactual data and ensure the reproducibility and translational fidelity of future in vitro pharmacological evaluations.

Introduction

Uterine leiomyomas (ULs), commonly known as fibroids, are the most prevalent benign tumors among reproductive-aged women, affecting up to 70% of this population [1–3]. Although typically non-malignant [4], ULs pose a major clinical challenge due to their high prevalence and substantial impact on women's health [5, 6]. Notably, ULs are linked to infertility and subfertility, contributing to impaired implantation, recurrent pregnancy loss, and adverse pregnancy outcomes [7–9]. With declining birth rates in many countries, addressing UL-related reproductive dysfunction has emerged as a critical public health priority.

Current treatment strategies for ULs are predominantly surgical, including myomectomy and hysterectomy, which may compromise fertility or may be unsuitable for women desiring future fertility [10]. Although pharmacological options such as hormone therapies and selective progesterone receptor modulators (SPRMs) have been explored, their clinical applications remain constrained by incomplete efficacy, side effects, and inconsistent therapeutic responses [11]. These limitations underscore the need for more effective, mechanism-based, and non-invasive therapeutic strategies, which inherently depend on the availability of highly reliable and reproducible experimental models.

At the molecular level, ULs are monoclonal tumors originating from myometrial smooth muscle cells [12, 13], characterized by excessive extracellular matrix (ECM) deposition and altered tissue architecture [14, 15]. Recurrent somatic mutations, particularly in *MED12*, and alterations in *HMGA2* expression and related pathways highlight the genetic heterogeneity of these tumors [16–18]. Additionally, UL growth is strongly hormone-dependent, with estrogen and progesterone regulating proliferation and ECM remodeling through receptor-mediated signaling pathways [19–22]. These features make ULs attractive targets for hormone-based and targeted therapeutic interventions, emphasizing the critical importance of utilizing models that accurately reflect these native molecular dependencies.

Primary two-dimensional (2D) culture systems are among the most widely utilized experimental platforms for investigating UL biology. These systems provide a practical and accessible framework for studying cell proliferation, hormone responsiveness, molecular signaling, and drug effects, and are particularly well-suited for high-throughput and mechanistic studies. However, despite their widespread use, the experimental conditions for primary UL cell culture vary considerably across studies (Table 1) [23–29]. Unstandardized variations in tissue dissociation methods, media composition, and passaging strategies significantly influence cell yield, growth dynamics, and molecular characteristics. This methodological heterogeneity severely compromises the reproducibility of experimental results and complicates the interpretation of in vitro findings across the field.

Table 1
Literature review of primary human UL cell culture parameters.

parameters	Shin SJ et al., 2018	Condon J et al., 2002	Suo G et al., 2009	Chang HL et al., 2010	Goad J et al., 2022	Ono M et al., 2007	Pandey V et al., 2019
Digestion enzyme	collagenase II	type I collagenase	collagenase II	type II collagenase	Liberase & Dispase	collagenase	collagenase type-1
Digestion time	4h	4h	3 ~ 5h		30 min	4–16 h	3h
Culture media	10% FBS, 1x P/S in DMEM	10% FBS, 10000 units/ml AA in DMEM/F-12	10% FBS, 1x P/S in DMEM			MSC growth medium	10% FBS, 1x AA in DMEM
Coating materials							
Detachment		trypsin-EDTA	trypsin				
* References cited in this table are listed in the Reference section							

Beyond this methodological variability, a more profound and underexplored challenge is the temporal stability of primary UL cells. It remains inadequately defined how long these cells retain their tissue-specific molecular identity under 2D culture conditions. The abrupt transition from a highly rigid, 3D native tumor microenvironment to a flat, plastic 2D surface deprives these cells of essential mechanical and spatial cues. Consequently, prolonged in vitro expansion inevitably drives culture-induced cellular adaptation and active transcriptional reprogramming, leading to the irreversible loss of their native identity [30]. This rapid loss of tissue identity not only introduces critical artifacts into molecular signaling studies but also critically distorts drug responsiveness evaluations, particularly in hormone-dependent contexts.

This study aimed to establish a comprehensive framework for optimizing and interpreting primary UL cell cultures using 2D systems. We systematically evaluated enzymatic dissociation methods, passaging strategies, and culture conditions, examining their effects on cell yield, proliferative capacity, gene expression profiles, and hormone- and drug-responsiveness over serial passages. Using this approach, we sought to define a biologically relevant culture window and identify the conditions that preserved the key functional features of UL cells within the practical advantages of 2D culture systems. This framework may facilitate reliable translation of *in vitro* findings into physiologically relevant contexts, providing an essential baseline for the development of advanced platforms, such as three-dimensional (3D) organoid models.

Results

Uterine leiomyoma tissues exhibit distinct histopathological features compared with normal myometrium.

Paired uterine leiomyomas (ULs) and adjacent normal myometrial tissues were obtained from three premenopausal women (aged 37–44 years) who underwent myomectomy or hysterectomy for symptomatic uterine fibroids (Table 2). The patients presented with variable clinical characteristics, including body mass index ranging from 25.3 to 29.3 kg/m², parity of 0–1, and fibroid size ranging from 4.0 to 13.0 cm. The lesions included intramural fibroids. One patient received preoperative gonadotropin-releasing hormone treatment. Molecular and histopathological evaluations revealed heterogeneity within the cohort. Two tumors were classified as conventional ULs, and one was diagnosed as an atypical smooth muscle tumor of uncertain malignant potential (STUMP). MED12 mutations were identified in three tumors, including c.130G > A (p.G44S) and c.131G > C (p.G44A), while one tumor had no defined mutation. Additionally, the STUMP case demonstrated high HMGA expression status together with a MED12 mutation. All diagnoses were histologically confirmed and none of the patients had malignant gynecological diseases.

Table 2
Clinical characteristics of patients with uterine fibroids

Patient	Age (years)	BMI (kg/m²)	Parity	Indication for surgery	Fibroid size (cm)	Fibroid location	Preoperative hormonal treatment	Type of surgery	Mutation type
UF-1	44	25.3	1	Uterine leiomyoma	5.2	Intramural	(-)	Myomectomy	Unknown
UF-2	39	26.2	0	Uterine leiomyoma	13	Intramural	GnRH 2 cycles	Myomectomy	MED12 c.130G > A (p.G44S)
STUMP	37	29.3	1	Uterine leiomyoma (STUMP)	4	Intramural	(-)	Hysterectomy	HMGA high & MED12 c.131G > C (p.G44A)
Footnotes:									
• All samples were obtained from premenopausal women.									
• Fibroid diagnosis was histologically confirmed.									
• None of the patients had malignant gynecologic disease.									
• The study was approved by the Institutional Review Board (IRB No. 2026-02-064) and was conducted in accordance with the 1964 Declaration of Helsinki and its later amendments or comparable ethical standards.									
• Written informed consent was obtained from all participants.									

Histological characteristics of ULs and the corresponding normal myometrial tissues were evaluated using hematoxylin and eosin (H&E) and Masson's trichrome staining (Fig. 1). On H&E staining (Fig. 1A), the normal myometrium exhibited well-organized smooth muscle bundles with uniform cellular architecture. In contrast, UL tissues from both the usual uterine fibroids (Usual UF-1 and UF-2) displayed disorganized and densely packed smooth muscle fascicles with altered tissue architecture. The STUMP sample demonstrated more irregular and heterogeneous structural features than usual UL tissues. Masson's trichrome staining (Fig. 1B) revealed differences in extracellular matrix organization between normal myometrial and UL tissues. The normal myometrium showed relatively limited and evenly distributed collagen deposition. Distinct patterns were observed among UL samples across cases. The usual UF-1 cells exhibited densely packed smooth muscle bundles with high cellularity, which resulted in a relative reduction in the proportion of collagen-stained regions. In contrast, the usual UF-2 cells showed increased heterogeneous collagen deposition. The STUMP sample demonstrated a mixed and disorganized distribution of collagen and smooth muscle components, indicating greater structural heterogeneity than usual leiomyoma tissues. Collectively, these findings demonstrate that the study cohort encompasses diverse clinical and molecular characteristics along with distinct histopathological features of UL tissues compared with normal myometrium. The observed heterogeneity, including differences between usual UF and STUMP, provides a relevant framework for subsequent analyses of primary UL-derived cells and their behavior under defined experimental conditions.

Initial enzymatic stress dictates early cellular recovery but is overridden by long term culture adaptation.

To establish primary cultures of UL-derived cells, three enzymatic dissociation protocols (E1–E3), selected based on previously reported methods for uterine tissue and smooth muscle cell isolation, were evaluated using patient-derived fibroid tissues, including usual UF and STUMP samples (Fig. 2A). It was confirmed that the enzymatic conditions influenced both the initial yield and the subsequent culture behavior of UL-derived cells (Fig. 2B). E1 digestion, based on collagenase type I, generated a

higher proportion of dispersed cells with minimal aggregation, whereas digestion with E2 (collagenase type II) and E3 (a commercial mixture of collagenase types I and II) resulted in incomplete tissue dissociation, characterized by the presence of extracellular matrix debris and a relative paucity of liberated cells across both the usual UF and STUMP samples. Moreover, E1 produced the highest number of viable cells immediately post-dissociation, whereas E2 and E3 produced fewer viable cells (Fig. 2C). Cells derived from E2 and E3 conditions exhibited extended culture durations compared to those obtained using E1 (Fig. 2D), indicating a divergence between the initial yield and subsequent culture persistence.

Subsequent analysis confirmed that the impact of enzymatic dissociation on cell yield and culture behavior were most prominent during the initial passages. Passages P0–P1, E1 yielded the highest number of viable cells while needing a shorter culture duration, whereas E2 and E3 produced fewer cells with relatively prolonged culture periods (Fig. 2E and F). As passaging progressed, cell numbers across all conditions became comparable, reflecting density-controlled passaging at defined confluency (Fig. 2E). Concurrently, differences in culture duration diminished over time, with all conditions exhibiting similar growth patterns after early passages (Fig. 2F). These results indicate that enzymatic dissociation primarily affects early cell yield and short-term culture behavior, with its influence become less pronounced during long-term culture, and can be mitigated by controlling cell density during passaging.

Enzymatic passaging confers a sustained advantage in cellular expansion and adherence under in vitro constraints.

To investigate the impact of passaging conditions on primary UL cell culture, cells isolated under E1–E3 conditions were cultured using either trypsin-EDTA (TE) or Gentle Cell Dissociation Reagent (GCDR). TE is routinely used for UL cell dissociation, whereas GCDR, a milder non-enzymatic reagent commonly used to preserve stem-like cell populations, was selected for comparison across serial passages. Given that UL is a clonal tumor and that the maintenance of stem-like cell populations may be critical during in vitro expansion, we further evaluated how these distinct dissociation approaches affect cell yield and culture behavior.

As shown in Fig. 3A, we observed morphological differences between the two passaging methods across all samples on day 5 of culture. Although cells were routinely passaged upon reaching approximately 80%–90% confluency, TE-treated cells exhibited a dense and well-spread morphology, whereas GCDR-treated cells displayed a more dispersed and less adherent phenotype. Quantitative analysis revealed that TE consistently yielded higher numbers of viable cells, approximately two-fold greater than those obtained with GCDR, across all samples and passages under the E1 conditions (Fig. 3B and C), indicating reduced detachment efficiency under non-enzymatic conditions. Furthermore, TE-treated cells achieved high confluence more rapidly than GCDR-treated cells, suggesting a relatively lower expansion capacity when employing the non-enzymatic method. Similar patterns were observed under E2 and E3 enzymatic conditions (Fig. 3D–G). Therefore, the choice of passaging method directly impacts cell expansion efficiency, with enzymatic dissociation offering a consistent advantage for cell recovery and growth during serial cultures.

Long-term passaging reveals progressive decline in cell expansion capacity and earlier growth arrest under non-enzymatic conditions.

With continued passaging, the culture dynamics increasingly diverged between the two detachment strategies. Representative images at later passages highlighted differences in long-term proliferative capacity (Fig. 4A). TE-treated cultures maintained relatively high confluency on day 5 of P7, whereas cell density was markedly reduced by P15. In some instances, sufficient cell growth was not achieved for image acquisition. In contrast, GCDR-treated cultures exhibited low confluency at P7, reflecting a limited proliferative capacity during relatively early passages.

Consistent with these observations, the cell yield progressively declined with increasing passage number under both passaging conditions, and this trend was consistently observed across cells derived from all dissociation conditions (E1–E3; Fig. 4B, D, F), with a more pronounced and earlier reduction in GCDR-treated cultures. Concurrently, the culture duration was prolonged during extended passaging, with GCDR-treated cells showing a more pronounced increase, frequently failing to reach the detachment threshold, and becoming non-expandable around P10–11. In comparison, TE-treated cultures exhibited a more gradual extension of culture intervals and remained expandable to later passages despite reduced yields at advanced passages.

Similar patterns were observed under the E2 and E3 enzymatic conditions (Fig. 4D–G), with progressive declines in cell density, prolonged culture duration, and reduced cell yield, consistent with those observed under the E1 condition. These results indicate that non-enzymatic dissociation leads to an earlier loss of expansion capacity during long-term culture, highlighting its limitations in sustained cell propagation.

Passaging strategy differentially affects gene expression profiles and stem-like marker maintenance in UL cells.

To evaluate the preservation of tissue-specific molecular characteristics in primary UL cells during 2D culture, we analyzed the expression of the smooth muscle marker *ACTA2* (α-smooth muscle actin, α-SMA), hormone receptors (*ESR1, PGR*), stemness-associated genes (*NANOG, POU5F1, SOX2*), and myometrial stemness surface markers (*CD34, CD44, ITGA2*) using quantitative polymerase chain reaction across tissue samples and serial passages. We first compared the gene expression profiles of matched normal myometrium (NM) and uterine fibroid (UF) tissues (Fig. 5A and Supplementary Fig. 1). Across the combined cohort, UF tissues displayed increased expression of multiple genes, including *ESR1* and *PGR*, indicating enhanced hormone responsiveness consistent with the hormone-dependent nature of uterine fibroids, as well as several stemness-associated markers compared with NM. In contrast, *ACTA2* expression exhibited variable patterns across individual cases, with no consistent differences between NM and UF at the cohort level (Fig. 5A and Supplementary Fig. 1). *CD34* expression was consistently reduced in UF tissues across all samples, indicating a reduced presence of CD34-positive cell populations and alterations in the cellular composition of fibroid tissues. *CD44* expression exhibited marked inter-sample variability, with decreased levels in usual UF-1, increased expression in usual UF-2, and pronounced elevation in the STUMP sample, indicating case-dependent heterogeneity and a potential association with enhanced stem-like features or extracellular matrix interactions in more atypical tumors. In contrast, *ITGA2* (encoding CD49b) expression displayed less consistent changes, with a significant increase observed only in UF-2, indicating a more context-dependent role in cell-matrix interactions rather than a uniform feature of fibroid tissues.

We subsequently compared the gene expression profiles of the UF and early-passage cells cultured under TE or GCDR detachment conditions (Fig. 5B). Upon transitioning from tissue status to 2D culture, substantial transcriptional changes were observed across most markers. *ACTA2* expression was partially preserved at P1, particularly in TE-cultured cells, but was markedly decreased by P2 under both conditions. In contrast, hormone receptor genes were rapidly downregulated; *ESR1* expression was nearly undetectable at P1, whereas *PGR* remained weakly expressed at P1, slightly higher in GCDR-treated cells, but almost completely lost at P2. Stemness-associated genes exhibit heterogeneous but transient responses. NANOG expression decreased sharply at P1 under both conditions, although relatively high levels were maintained in the GCDR-treated cells. In contrast, *POU5F1* (commonly known as OCT4) and *SOX2* were transiently upregulated at P1 under GCDR conditions, exceeding the levels observed in UF tissues, followed by a pronounced reduction at P2. TE-cultured cells did not exhibit comparable induction. Surface marker expression further highlighted the early divergence from tissue profiles. *CD34* expression decreased markedly at P1 and was largely lost at P2 under both conditions. In contrast, *CD44* and *ITGA2* were upregulated at P1, particularly in GCDR-treated cells, and remained detectable at P2, despite a partial reduction. These trends were derived from the combined cohort analysis. Individual patient-level data are provided in Supplementary Fig. 2, showing broadly consistent patterns across samples with some degree of interpatient variability. These results indicate that primary UL cells undergo rapid transcriptional remodeling upon adaptation to 2D culture, with non-enzymatic dissociation providing limited and transient preservation of selected stemness- and adhesion-related markers, while ultimately failing to preserve the native molecular characteristics of UL tissues.

To further assess passage-dependent transcriptional changes, we analyzed gene expression patterns across early passages (P2–P5) relative to P1 using a heatmap-based visualization (Fig. 5C). Consistent with the rapid remodeling observed in the early culture stages, most tissue-specific gene expression patterns showed progressive divergence from the P1 baseline during subsequent passaging. Smooth muscle marker expression declined rapidly, with *ACTA2* levels being markedly reduced from P4 onward. Similarly, the hormone receptor genes *ESR1* and *PGR* showed a sharp decrease beginning at P3, indicating an early loss of hormone-responsive characteristics. In contrast, stemness-associated markers displayed more heterogeneous dynamics, with partial recovery or stabilization observed over time following an initial decline at early passages. Surface marker expression exhibited variable patterns across the genes. *CD44* expression decreased rapidly during early passages,

whereas *CD34* and *ITGA2* displayed fluctuating, nonuniform changes across passages without a consistent trend. These results indicate that transcriptional instability is established during early passages, with gene-specific patterns of decline or adaptation.

At later passages, we examined gene expression patterns relative to P1 to assess the extent of transcriptional changes during prolonged culture (Fig. 5D). Consistent with progressive transcriptional drift, *ESR1* expression continued to decline over time and became negligible beyond P10, indicating a near-complete loss of ER-associated signaling during long-term culture. In contrast, *PGR* expression exhibited a distinct pattern with an initial decrease, followed by partial re-emergence from approximately P11, suggesting context-dependent reactivation or selective enrichment of *PGR*-expressing cell populations during prolonged passaging. The expression of surface markers also exhibited dynamic changes. *CD34* expression remained consistently low across late passages, indicating sustained depletion of CD34-positive cell populations. In contrast, *CD44* and *ITGA2* showed a gradual increase at later passages, followed by an earlier decline, suggesting adaptive changes in cell adhesion or extracellular matrix interactions during long-term culture. These findings indicate that prolonged 2D culture not only drives the loss of tissue-specific gene expression but also induces adaptive transcriptional reprogramming. Collectively, these results demonstrate that primary UL cells rapidly lose tissue-specific molecular characteristics during 2D culture, with progressive transcriptional drift and partial reprogramming occurring upon continued passaging. Although nonenzymatic dissociation provides transient preservation of selected stemness- and adhesion-related markers, these effects remain limited and do not prevent the overall loss of native molecular identity.

Optimized culture conditions partially restore cell expansion and hormone responsiveness in UL cells.

To address the rapid loss of tissue-specific molecular characteristics observed upon adaptation to 2D culture, including a marked reduction in *ESR1*, *PGR*, and stemness-associated markers (Fig. 5), we established a manually formulated culture medium (CM) by incorporating components commonly used to support epithelial or mesenchymal stem-like cell maintenance, stress resistance, and controlled cell expansion (Fig. 6A). Compared with the conventional serum-containing complete medium (C), comprising DMEM/F-12 supplemented with 10% FBS and antibiotics, the CM contained B27, N2, GlutaMAX, and non-essential amino acids to support cell maintenance under lower-serum conditions. EGF and R-spondin-1 were added to promote survival and proliferative signaling, while Noggin and A83-01 were included to modulate BMP and TGF-β/ALK signaling, respectively, while NAC was incorporated to reduce oxidative stress during serial culture. We compared this CM formulation with the C medium to determine whether a more defined, stem-supportive condition could improve expansion and preserve the molecular and functional features of primary UL-derived cells.

We observed that cells cultured in CM exhibited a more compact, tissue-like architecture, characterized by increased cell density and organized whorl-like growth patterns, compared to those cultured in C medium (Fig. 6B). These features were most evident at early passages, when CM-cultured cells displayed a more pronounced smooth muscle-like morphology. Consistent with these observations, the CM medium supported enhanced cell expansion during early passages (P3–P5), resulting in a higher cell yield than the C medium. However, this advantage was not sustained, as CM cultures showed reduced confluency and a marked decline in cell yield from later passages onward, eventually falling below those observed in C-cultured cells (data are not shown).

Gene expression analysis further elucidated the passage-dependent effects of CM conditions (Fig. 6C). During early passages (P2), CM-cultured cells exhibited increased expression of multiple markers, including *ESR1*, *PGR*, and surface markers such as *CD44* and *ITGA2*, compared to the C medium. In contrast, *ACTA2* and *CD34* levels showed limited or no improvement under CM conditions. At later passages (P6), the CM-cultured cells showed a broad reduction in gene expression, with levels decreasing below those observed in the C-cultured cells. These findings indicate that the CM-mediated preservation of molecular characteristics is transient and largely confined to early passages.

Subsequently, we evaluated whether the partial restoration of *ESR1* and *PGR* expression in CM translated into functional hormone responsiveness (Fig. 6D). While estradiol (E2) alone did not induce a marked difference between the conditions, progesterone (P4) treatment led to a modest increase in the cellular response in CM-cultured cells, which was further enhanced by combined E2 and P4 stimulation, suggesting altered hormone responsiveness under CM conditions during early passages.

Given that SPRMs act through progesterone receptor signaling, subsequent drug response experiments were performed with or without P4 to specifically evaluate PR-dependent effects. To investigate how differences in culture medium and hormone availability influence cellular responses to SPRMs, we assessed cell viability under hormone-present and -deprived conditions (Fig. 6E and F). Cellular responses vary depending on hormone availability and culture conditions. In the absence of progesterone, most SPRMs exhibited minimal effects under both media conditions, although bazedoxifene (Baze) exerted a stronger inhibitory effect under condition C. In the presence of hormones, cells cultured in C medium responded to both ulipristal acetate (UPA) and Baze, whereas CM-cultured cells exhibited a more restricted response, with significant sensitivity to Baze. These findings indicate that SPRM responsiveness is strongly influenced by both hormonal context and culture conditions, with CM conditions enabling more hormone-dependent and context-specific responses. Collectively, these results show that optimization of culture conditions modulates the phenotypic and functional behavior of primary UL cells in a passage-dependent manner, with improvements observed at early passages but not maintained during prolonged culture.

Discussion

Uterine leiomyomas (ULs) constitute a significant unmet clinical challenge, particularly regarding fertility preservation and the development of effective, non-invasive therapies. The limited efficacy and variability of current treatment modalities underscore the critical need for improved therapeutic strategies, which inherently depend on reliable experimental models for mechanistic evaluation and drug screening. While primary two-dimensional (2D) culture systems are extensively employed, unstandardized experimental conditions and a poor understanding of passage-dependent phenotypic drift severely compromise the reproducibility and interpretability of in vitro findings. In the present study, we systematically evaluated key methodological variables and integrated patient-specific heterogeneity with longitudinal analyses to establish a definitive framework for primary UL cell culture. By defining the biologically relevant "culture window," this framework not only improves the translational fidelity of 2D UL models but also establishes an essential foundational baseline for the development of advanced, physiologically relevant platforms, such as three-dimensional (3D) organoid systems.

The patient samples analyzed in this study exhibited substantial clinical, histological, and molecular heterogeneity, reflecting the intrinsic biological complexity of ULs. Even within the same molecular subcategories, such as tumors harboring MED12 mutations, we observed pronounced variability in extracellular matrix (ECM) organization and smooth muscle cellularity. Furthermore, the STUMP case, characterized by both a MED12 mutation and elevated HMGA2 expression, displayed a markedly disorganized tissue architecture. This profound intra- and inter-tumoral heterogeneity makes the standardization of early culture conditions absolutely critical to distinguish true tumor biology from experimental artifacts. When evaluating tissue dissociation protocols, we found that despite differences in native tissue composition, collagenase type I (E1) provided a remarkably robust and broadly applicable strategy, consistently yielding the highest initial recovery of viable cells across all samples. This high efficiency is likely because ULs are universally enriched in type I collagen and extracellular matrix components [31], making them particularly susceptible to collagenase type I-mediated degradation. These findings demonstrate that while the chosen dissociation enzyme dictates early cellular recovery, standardized downstream culture conditions effectively mitigate initial variability, ultimately providing a reproducible platform that supports stable expansion while accommodating underlying biological diversity.

Following initial tissue dissociation, the choice of detachment method during serial passaging exerted a profound effect on the long-term expansion capacity and stability of primary UL cells. While non-enzymatic reagents like GCDR are frequently employed to preserve stem-like cell populations, our longitudinal data revealed that this approach resulted in inefficient detachment and consequently lower effective seeding densities. This technical limitation necessitated extended culture intervals to achieve confluency, which likely imposed cumulative proliferative stress on the cells, thereby accelerating the onset of growth arrest and a senescence-like state. In contrast, enzymatic passaging with trypsin-EDTA (TE) facilitated more efficient recovery and sustainable expansion. However, even under optimized TE conditions, the proliferative capacity inevitably declined during long-term culture. This trajectory highlights that while passaging strategies can modulate expansion kinetics, 2D propagation inherently imposes a finite limit on primary UL cell survival, necessitating careful monitoring of culture duration.

The profound biological limitations of prolonged 2D expansion are most starkly reflected in the rapid transcriptional drift and loss of tissue-specific molecular identity. Upon transitioning from the native tumor microenvironment to rigid 2D monolayers, UL cells underwent immediate and extensive phenotypic reprogramming. Hormone receptor signaling proved exceptionally vulnerable to the absence of native microenvironmental cues, evidenced by the precipitous decline in *ESR1* and *PGR* expression as early as passages 1 and 2, which was closely followed by the progressive loss of the smooth muscle marker *ACTA2*. Although the milder GCDR detachment provided a transient preservation of select stemness (*POU5F1, SOX2*) and adhesion (*CD44, ITGA2*) markers, it failed to halt the overarching trajectory of dedifferentiation. This rapid transcriptomic remodeling aligns with observations in other primary cell systems, where the absence of physiological mechanical cues, native ECM, and three-dimensional architecture collectively drives a shift from a highly differentiated phenotype toward a proliferative, unspecialized state [32–37].

Crucially, our longitudinal profiling indicates that prolonged 2D culture does not simply induce a uniform loss of UL characteristics, but rather drives a selective adaptation that favors cellular states optimized for survival in vitro. Notably, while essential tumor-specific drivers diminished, adhesion-related markers such as *CD44* and *ITGA2* exhibited dynamic expression patterns that ultimately converged toward tissue baseline levels. This selective preservation suggests a cellular prioritization of substrate attachment to cope with the mechanical constraints of rigid plastic dishes, potentially linked to early replicative senescence [38–41]. Consequently, extended serial passaging actively enriches for culture-adapted subpopulations that bear little resemblance to the original in vivo tumor biology. These findings definitively establish that only the earliest passages represent a pathophysiologically valid "culture window." Utilizing cells beyond this critical timeframe fundamentally distorts experimental outcomes, yielding artefactual data driven by in vitro selection pressures rather than intrinsic leiomyoma pathology.

Within the context of this progressive transcriptional drift, optimizing culture media emerged as a modulatory, rather than curative, intervention. While our optimized formulation (CM) transiently enhanced early cell expansion and partially preserved hormone responsiveness, it ultimately failed to halt the inexorable decline of key leiomyoma-associated markers, including ACTA2 and hormone receptors. This underscores a fundamental biological reality: defined soluble factors and signaling modulators cannot adequately substitute for the physiological mechanical cues and native ECM interactions required to sustain cellular differentiation. As a result, the pharmacological evaluation of UL cells is highly vulnerable to these culture-induced adaptations. As demonstrated by the highly variable sensitivity to selective progesterone receptor modulators (SPRMs) across different media and hormonal contexts, drug responsiveness in 2D culture is not dictated solely by intrinsic tumor biology, but is profoundly distorted by the cellular adaptation to the in vitro environment. Our findings align with previous observations that drug responses are shaped by dynamic interactions between intrinsic tumor biology and culture-induced cellular states [42]. Therefore, pharmacological evaluation in primary UL models must be strictly confined to the early-passage window, as testing outside this timeframe risks generating entirely artefactual data that lacks clinical translatability.

We acknowledge certain limitations in this study, including the restricted patient cohort (n = 3) and the inherent physiological constraints of a conventional 2D system. Additionally, transcriptomic evaluations were confined to targeted markers rather than global profiling. However, these limitations precisely reinforce the central thesis of our work: the transcriptomic and functional shifts observed here are not intrinsic tumor progression, but rather severe culture-induced adaptations. By systematically defining the extent, timing, and drivers of this phenotypic drift, our study establishes a definitive, biologically relevant "culture window" for primary 2D UL models. Recognizing that experimental outcomes are shaped by dynamic interactions between native tumor biology and externally imposed in vitro pressures is paramount for ensuring the reproducibility and translational fidelity of future pharmacological studies. Ultimately, the standardized framework and the explicit limitations of 2D cultures identified here form an indispensable baseline, urgently underscoring the necessity to transition toward advanced, physiologically representative models, such as three-dimensional (3D) organoids, to truly capture the complexity of hormone-dependent reproductive diseases.

Methods

Patient tissue collection. Human UL tissue specimens were obtained from patients undergoing myomectomy or hysterectomy at Dongsan Medical Center (Daegu, Republic of Korea). A total of three women aged 19–49 years who underwent surgery for symptomatic ULs between August and September 2025 were included in this study. Written informed consent was obtained from all participants prior to surgery, and the study protocol was approved by the Institutional Review Board of Dongsan Medical Center (Daegu, Republic of Korea; approval no. 2026-02-064) and was conducted in accordance with the 1964 Declaration of Helsinki and its later amendments or comparable ethical standards. All collected specimens were histopathologically reviewed and confirmed as UL by a board-certified pathologist. When available, paired myometrial tissue located at a distance from the UL was collected from the same patient and used as a control. Fresh tissue samples were collected immediately after surgical resection and placed in ice-cold HBSS (Welgene Inc., Daegu, South Korea). A small part of each tissue was snap-frozen to isolate DNA or RNA for detection the presence of the MED12 variants, FH mutations, or HMGA2 overexpression. Additionally, a part of the sample was fixed in 4% PFA (Biosesang, Seongnam, South Korea) for histology.

Gelatin embedding and frozen tissue preparation. Fixed tissues were cryoprotected by incubation in 30% sucrose in PBS overnight at 4°C. On the following day, tissues were incubated in a gelatin solution (7.5% gelatin, 10% sucrose in PBS) at 37°C until fully infiltrated. Infiltrated tissues were then placed onto pre-solidified cold gelatin blocks and allowed to partially solidify. Additional gelatin solution was subsequently added to fully cover the tissues, and the blocks were further solidified at 4 ℃. The gelatin-embedded tissues were rapidly frozen in 2-methylbutane (Sigma-aldrich, St. Louis, MO, USA) pre-cooled at -80 ℃ and stored at -80 ℃ until sectioning. Frozen blocks were cryo-sectioned at a thickness of 20 μm using a cryostat (HM525NX; Thermo Fisher Scientific, Waltham, MA, USA) and sections were mounted onto the Superfrost™ Plus Microscope Slides (Fisher Scientific, Carlsbad, CA). Prepared slides were stored at -80 ℃ until further use.

Isolation of uterine leiomyoma cells. To determine the optimal conditions for the isolation of UL cells, tissues were cut into small pieces approximately 2–3 mm in size and divided equally into three portions. Each portion was incubated with 10 ml of enzyme solution (E1, E2, E3). Protocol E1 consisted of 2 mg/ml type I collagenase (Gibco, Waltham, MA, USA) and 0.5 mg/ml Dispase (Gibco, Waltham, MA, USA) and 0.1 mg/ml DNase-I (Sigma-aldrich, St. Louis, MO, USA) in HBSS (Welgene Inc., Daegu, South Korea). Protocol E2 consisted of 0.4% type II collagenase (Gibco, Waltham, MA, USA) and 6.5 mg/ml HEPES (Welgene Inc., Daegu, South Korea) and 0.1 mg/ml DNase-1 (Sigma-aldrich, St. Louis, MO, USA) in HBSS (Welgene Inc., Daegu, South Korea). Protocol E3 consisted of 0.1 mg/ml Liberase TL (Merck, Darmstadt, Germany) and 0.1 mg/ml DNase-I (Sigma-aldrich, St. Louis, MO, USA) in HBSS (Welgene Inc., Daegu, South Korea). The samples were subjected to enzymatic digestion at 37 ℃ with continuous rotation until the tissue was sufficiently digested and dispersed into single cells. Following dissociation, the cell suspensions were filtered through a 70 μm cell strainer, and 10 ml of culture medium was added to terminate the enzymatic reaction. Cells were then harvested and centrifuged to remove debris and washed with fresh medium. After centrifugation, the cell pellet was resuspended in culture medium, and cell yield was quantified by trypan blue exclusion-based cell counting using Countess 3 Automated Cell Counter (Thermo Fisher Scientific, Waltham, MA, USA) before seeding. Finally, the isolated cells were seeded onto cell culture dishes coated with 1% Matrigel (Corning, NY, USA) in DMEM/F-12 (Gibco, Waltham, MA, USA).

Culture of primary UL cells. Cells were maintained at 37 ℃ in a humidified incubator with 5% CO_2. To evaluate which detachment reagent better preserves original cell identity during long-term culture, cells were continuously passaged using either trypsin–EDTA (0.25%; Welgene Inc., Daegu, South Korea) or Gentle Cell Dissociation Reagent (GCDR; STEMCELL Technologies, Vancouver, Canada) when cultures reached approximately 80–90% confluency. At each passage, cell yield and the duration required to reach the subsequent passage were recorded, bright-field images were acquired, and cell samples were collected at each passage for subsequent quantitative PCR (qPCR) analysis to assess the maintenance of stem-like cell populations as well as the expression of lineage- and hormone receptor–related markers. To determine optimal culture conditions, two different media formulations were used. The conventional serum-containing complete medium (C) consisted of DMEM/F12 medium (Gibco, Waltham, MA, USA) supplemented with 10% FBS (Gibco, Waltham, MA, USA) and 1X antibiotic-antimycotic solution (GenDepot, Katy, TX, USA). The manually formulated culture medium (CM) was prepared using DMEM/F12 medium (Gibco, Waltham, MA, USA) supplemented with 0.5X B27 supplement (Gibco, Waltham, MA, USA), 0.5X N2 supplement (Gibco, Waltham, MA, USA), 0.5X GlutaMAX (Gibco, Waltham, MA, USA), 0.5X non-essential amino acids (NEAA; Gibco, Waltham, MA, USA), 10 ng/ml recombinant human epidermal growth factor (rhEGF; R&D, Minneapolis, MN, USA), 250 ng/ml

human R-spondin (PeproTech, Rocky Hill, NJ, USA), 250 nM A83-01 (Sigma-aldrich, St. Louis, MO, USA), 50 ng/ml human Noggin (PeproTech, Rocky Hill, NJ, USA), 0.5 mM N-acetylcysteine (NAC; Sigma-aldrich, St. Louis, MO, USA), 5% FBS (Gibco, Waltham, MA, USA), and 0.5X antibiotic–antimycotic solution (GenDepot, Katy, TX, USA). Cells cultured in C and CM were analyzed in parallel using the same experimental workflow, including acquisition of bright-field images, measurement of cell yield and culture duration, sampling for qPCR analysis, and hormone or drug treatment assays.

Cell viability assay. Cells were seeded in a 1% Matrigel-coated 96-well plate for 24h, and then treated with non-treated control (NT, DMSO 0.1%), β-estradiol (E2, 100 nM; Sigma-Aldrich, St. Louis, MO, USA), progesterone (P4, 100 nM), E2 + P4 (each 100 nM), ulipristal acetate (UPA), vilaprisan (Vila), bazedoxifene (Baze), (MedChemExpress, Monmouth Junction, NJ, USA) at a final concentration of 10 μM for 72h. Cell viability was measured by EZ-Cytox cell viability assay kit (DoGenBio, Seoul, South Korea) according to the manufacturer's instructions.

Genomic DNA extraction and PCR for detection of MED12 and FH mutation. Genomic DNA was extracted from fresh frozen tissue sample with GenEX™ tissue kit (GeneAll, Seoul, South Korea) according to the manufacturer's instructions. For PCR amplifications 50–100 ng of genomic DNA was used as a template and primers used to amplify the PCR fragment are listed in Supplementary Table 1. MED12 and FH mutation screening were performed by direct sequencing.

RNA extraction and reverse transcription-quantitative polymerase chain reaction (RT-qPCR) analysis. Total RNA was isolated from myometrial tissues, UL tissues, and UL cells using Hybrid R (GeneAll, Seoul, South Korea) according to the manufacturer's instructions. Equal amounts of RNA were used for RT-qPCR analysis. Reverse transcription was performed using cDNA synthesis master mix (LeGene Biosciences, San Diego, CA, USA) according to the manufacturer's instructions. qPCR was performed for *ACTA2* (α-SMA), *ESR1, PGR, NANOG, POU5F1*, *SOX2, CD34, CD44*, and *ITGA2* with primer sets listed in Supplementary Table 2, using iQ SYBR Green Master Mix (Bio-Rad, Hercules, CA, USA). The relative gene expression was normalized to *GAPDH* expression.

Hematoxylin and eosin (H&E) staining. Frozen tissue sections were removed from − 80°C storage and immediately transferred to ethanol to prevent drying and to achieve fixation. Sections were then subjected to standard hematoxylin and eosin (H&E) staining procedure. Briefly, sections were stained with hematoxylin (4min), rinsed in running tap water, differentiated with HCl alcohol as appropriate, followed by counterstaining with eosin to visualize the cytoplasm. After staining, sections were dehydrated through a graded ethanol series, cleared in xylene, and mounted with a mounting medium (Synthetic Mount/Shandon). Stained sections were imaged using an automatic slide scanner (Aperio GT 450, Leica Biosystems) for histological evaluation.

Masson's trichrome staining. Frozen tissue sections were removed from − 80°C and directly immersed in ethanol, followed by Masson's trichrome staining according to the manufacturer's instructions. Briefly, sections were sequentially stained with Weigert's iron hematoxylin (10min), Biebrich scarlet–acid fuchsin (10min), phosphomolybdic/phosphotungstic acid (10min), and aniline blue (10min) to visualize muscle fibers and collagen deposition. As the final step, acetic acid was applied (10 min) with washing in distilled water for 5 min between each step. Images were acquired using an automatic slide scanner (Aperio GT 450, Leica Biosystems).

Statistical analysis. Data are presented as mean ± standard error of the mean (SEM). Statistical analyses were performed using GraphPad Prism software. Comparisons between two groups were conducted using a two-tailed Student's *t*-test, while multiple-group comparisons were analyzed using two-way analysis of variance (ANOVA), as appropriate. A P value < 0.05 was considered statistically significant.

Declaration on the Use of Large Language Models. During the preparation of this manuscript, the authors used ChatGPT (OpenAI) or Gemini (Google) solely for language editing and text formatting. The authors critically reviewed all generated suggestions and retain full accountability for the originality and accuracy of the final content.

Declarations

Acknowledgements

The authors thank the clinicians and surgical staff of the Department of Obstetrics and Gynecology, Keimyung University Dongsan Medical Center, for their assistance in patient recruitment and the collection of UL and matched myometrial tissues. We also acknowledge the support of the institutional core facilities of the Department of Pathology for assistance with imaging and quantitative analysis.

Author's roles

N.K. participated in study design, performed the experiments, conducted data analysis, and drafted the manuscript. B.-R.C. and H.-R.J. contributed to histological experiments, data analysis, and interpretation. H.H. conceived and designed the study, supervised experimental execution and data analysis, and contributed to manuscript drafting and critical discussion. C.-H.C. served as principal investigator, contributed to study design, provided clinical samples, and participated in data interpretation and critical discussion. All authors reviewed and approved the final manuscript.

Funding

This work was supported by the Korea Medical Device Development Fund grant funded by the Korea government (Ministry of Health & Welfare, RS-2025-02214164) and a Bisa Research Grant from Keimyung University in 2015.

Competing Interests

The authors declare no conflict of interest.

Ethics approval

The study protocol was approved by the Institutional Review Board of Dongsan Medical Center (approval no. 2026-02-064) and was conducted in accordance with the 1964 Declaration of Helsinki and its later amendments or comparable ethical standards.

Data Availability

The datasets used and/or analysed during the current study are available from the corresponding author on reasonable request.

References

1. Baird, D. D., Dunson, D. B., Hill, M. C., Cousins, D. & Schectman, J. M. High cumulative incidence of uterine leiomyoma in black and white women: ultrasound evidence. *Am. J. Obstet. Gynecol.* **188**, 100–107 (2003).
2. Stewart, E. A., Cookson, C. L. & Gandolfo, R. A. Schulze-Rath, R. Epidemiology of uterine fibroids: a systematic review. *BJOG* **124**, 1501–1512. 10.1111/1471-0528.14640 (2017).
3. Stewart, E. A., Cookson, C. & Gandolfo, R. A. Schulze-Rath, R. Epidemiology of uterine fibroids: a systematic review. *BJOG: Int. J. Obstet. Gynecol.* **124**, 1501–1512 (2017).
4. Parker, W. H. Etiology, symptomatology, and diagnosis of uterine myomas. *Fertil. Steril.* **87**, 725–736. 10.1016/j.fertnstert.2007.01.093 (2007).
5. Barjon, K., Kahn, J. & Singh, M. *in StatPearls [Internet]* (StatPearls Publishing, 2025).
6. Gulersen, M., Krantz, D., Rochelson, B., Berghella, V. & Blitz, M. J. The association between uterine fibroid number and size and risk of preterm birth. *Am. J. Obstet. Gynecol. MFM*. **6**, 101415 (2024).
7. Cook, H., Ezzati, M., Segars, J. H. & McCarthy, D. The impact of uterine leiomyomas on reproductive outcomes. *Minerva Ginecol.* **62**, 225 (2010).
8. Donnez, J. & Jadoul, P. What are the implications of myomas on fertility? A need for a debate? *Hum. Reprod.* **17**, 1424–1430 (2002).

9. Pritts, E. A., Parker, W. H. & Olive, D. L. Fibroids and infertility: an updated systematic review of the evidence. *Fertil. Steril.* **91**, 1215–1223. 10.1016/j.fertnstert.2008.01.051 (2009).
10. Micić, J. et al. Currently available treatment modalities for uterine fibroids. *Medicina* **60**, 868 (2024).
11. Murji, A., Whitaker, L., Chow, T. L. & Sobel, M. L. *Selective progesterone receptor modulators (SPRMs) for uterine fibroids* (Cochrane Database of Systematic Reviews, 2017).
12. Mashal, R. D. et al. Analysis of androgen receptor DNA reveals the independent clonal origins of uterine leiomyomata and the secondary nature of cytogenetic aberrations in the development of leiomyomata. *Genes Chromosom. Cancer*. **11**, 1–6 (1994).
13. Townsend, D. E., Sparkes, R., Baluda, M. C. & McClelland, G. Unicellular histogenesis of uterine leiomyomas as determined by electrophoresis of glucose-6-phosphate dehydrogenase. *Am. J. Obstet. Gynecol.* **107**, 1168–1173 (1970).
14. Leppert, P. C. et al. Comparative ultrastructure of collagen fibrils in uterine leiomyomas and normal myometrium. *Fertil. Steril.* **82**, 1182–1187 (2004).
15. Stewart, E. A. et al. Uterine fibroids. *Nat. Rev. Dis. Primers*. **2**, 16043. 10.1038/nrdp.2016.43 (2016).
16. Ayravainen, A. et al. Systematic molecular and clinical analysis of uterine leiomyomas from fertile-aged women undergoing myomectomy. *Hum. Reprod.* **35**, 2237–2244. 10.1093/humrep/deaa187 (2020).
17. Bertsch, E. et al. MED12 and HMGA2 mutations: two independent genetic events in uterine leiomyoma and leiomyosarcoma. *Mod. Pathol.* **27**, 1144–1153. 10.1038/modpathol.2013.243 (2014).
18. Makinen, N., Kampjarvi, K., Frizzell, N., Butzow, R. & Vahteristo, P. Characterization of MED12, HMGA2, and FH alterations reveals molecular variability in uterine smooth muscle tumors. *Mol. Cancer*. **16**, 101. 10.1186/s12943-017-0672-1 (2017).
19. Kim, J. J. & Sefton, E. C. The role of progesterone signaling in the pathogenesis of uterine leiomyoma. *Mol. Cell. Endocrinol.* **358**, 223–231. 10.1016/j.mce.2011.05.044 (2012).
20. Milewska, G. et al. Functional evidence for two distinct mechanisms of action of progesterone and selective progesterone receptor modulator on uterine leiomyomas. *Fertil. Steril.* **122**, 341–351. 10.1016/j.fertnstert.2024.02.046 (2024).
21. Moravek, M. B. et al. Ovarian steroids, stem cells and uterine leiomyoma: therapeutic implications. *Hum. Reprod. Update*. **21**, 1–12. 10.1093/humupd/dmu048 (2015).
22. Reis, F. M., Bloise, E. & Ortiga-Carvalho, T. M. Hormones and pathogenesis of uterine fibroids. *Best Pract. Res. Clin. Obstet. Gynaecol.* **34**, 13–24. 10.1016/j.bpobgyn.2015.11.015 (2016).
23. Chang, H. L. et al. Uterine leiomyomas exhibit fewer stem/progenitor cell characteristics when compared with corresponding normal myometrium. *Reprod. Sci.* **17**, 158–167. 10.1177/1933719109348924 (2010).
24. Condon, J. et al. Telomerase immortalization of human myometrial cells. *Biol. Reprod.* **67**, 506–514 (2002).
25. Goad, J. et al. Single-cell sequencing reveals novel cellular heterogeneity in uterine leiomyomas. *Hum. Reprod.* **37**, 2334–2349. 10.1093/humrep/deac183 (2022).
26. Ono, M. et al. Side population in human uterine myometrium displays phenotypic and functional characteristics of myometrial stem cells. Proceedings of the National Academy of Sciences 104, 18700–18705 (2007).
27. Pandey, V., Rani, A. & Dubey, P. K. Uterine fibroid: Isolation, culture and characterization. *J. Biol. Eng. Res. Rev.* **6**, 27–31 (2019).
28. Shin, S. J. et al. Ulipristal acetate induces cell cycle delay and remodeling of extracellular matrix. *Int. J. Mol. Med.* **42**, 1857–1864 (2018).
29. Suo, G., Jiang, Y., Cowan, B. & Wang, J. Y. Platelet-derived growth factor C is upregulated in human uterine fibroids and regulates uterine smooth muscle cell growth. *Biol. Reprod.* **81**, 749–758. 10.1095/biolreprod.109.076869 (2009).
30. Zaitseva, M., Vollenhoven, B. J. & Rogers, P. A. In vitro culture significantly alters gene expression profiles and reduces differences between myometrial and fibroid smooth muscle cells. *Mol. Hum. Reprod.* **12**, 187–207 (2006).
31. Leppert, P. C., Jayes, F. L. & Segars, J. H. The extracellular matrix contributes to mechanotransduction in uterine fibroids. Obstet Gynecol Int. 783289, (2014). 10.1155/2014/783289 (2014).

32. Caron, M. M. et al. Redifferentiation of dedifferentiated human articular chondrocytes: comparison of 2D and 3D cultures. *Osteoarthr. Cartil.* **20**, 1170–1178. 10.1016/j.joca.2012.06.016 (2012).
33. Chang, S. et al. Phenotypic modulation of primary vascular smooth muscle cells by short-term culture on micropatterned substrate. *PLoS One*. **9**, e88089. 10.1371/journal.pone.0088089 (2014).
34. Dall, M., Stocks, B., Cervone, D. T., Deshmukh, A. S. & Treebak, J. T. Hepatocyte dedifferentiation in 2D culture reveals extensive transcriptomic and proteomic rewiring. *Hepatol. Commun.* **9** 10.1097/HC9.0000000000000795 (2025).
35. Pei, M. & He, F. Extracellular matrix deposited by synovium-derived stem cells delays replicative senescent chondrocyte dedifferentiation and enhances redifferentiation. *J. Cell. Physiol.* **227**, 2163–2174. 10.1002/jcp.22950 (2012).
36. Ghosh, S. et al. Dedifferentiation alters chondrocyte nuclear mechanics during in vitro culture and expansion. *Biophys. J.* **121**, 131–141. 10.1016/j.bpj.2021.11.018 (2022).
37. Sandison, M. E., Dempster, J. & McCarron, J. G. The transition of smooth muscle cells from a contractile to a migratory, phagocytic phenotype: direct demonstration of phenotypic modulation. *J. Physiol.* **594**, 6189–6209. 10.1113/JP272729 (2016).
38. Adorno-Cruz, V. & Liu, H. Regulation and functions of integrin alpha2 in cell adhesion and disease. *Genes Dis.* **6**, 16–24. 10.1016/j.gendis.2018.12.003 (2019).
39. Lee, J. L., Wang, M. J., Sudhir, P. R. & Chen, J. Y. CD44 engagement promotes matrix-derived survival through the CD44-SRC-integrin axis in lipid rafts. *Mol. Cell. Biol.* **28**, 5710–5723. 10.1128/MCB.00186-08 (2008).
40. Ponta, H., Sherman, L. & Herrlich, P. A. CD44: from adhesion molecules to signalling regulators. *Nat. Rev. Mol. Cell Biol.* **4**, 33–45 (2003).
41. Felisbino, M. B. et al. Substrate stiffness modulates cardiac fibroblast activation, senescence, and proinflammatory secretory phenotype. *Am. J. Physiol. Heart Circ. Physiol.* **326**, H61–H73. 10.1152/ajpheart.00483.2023 (2024).
42. Ayuso, J. M. et al. Effects of culture method on response to EGFR therapy in head and neck squamous cell carcinoma cells. *Sci. Rep.* **9**, 12480 (2019).

Figures

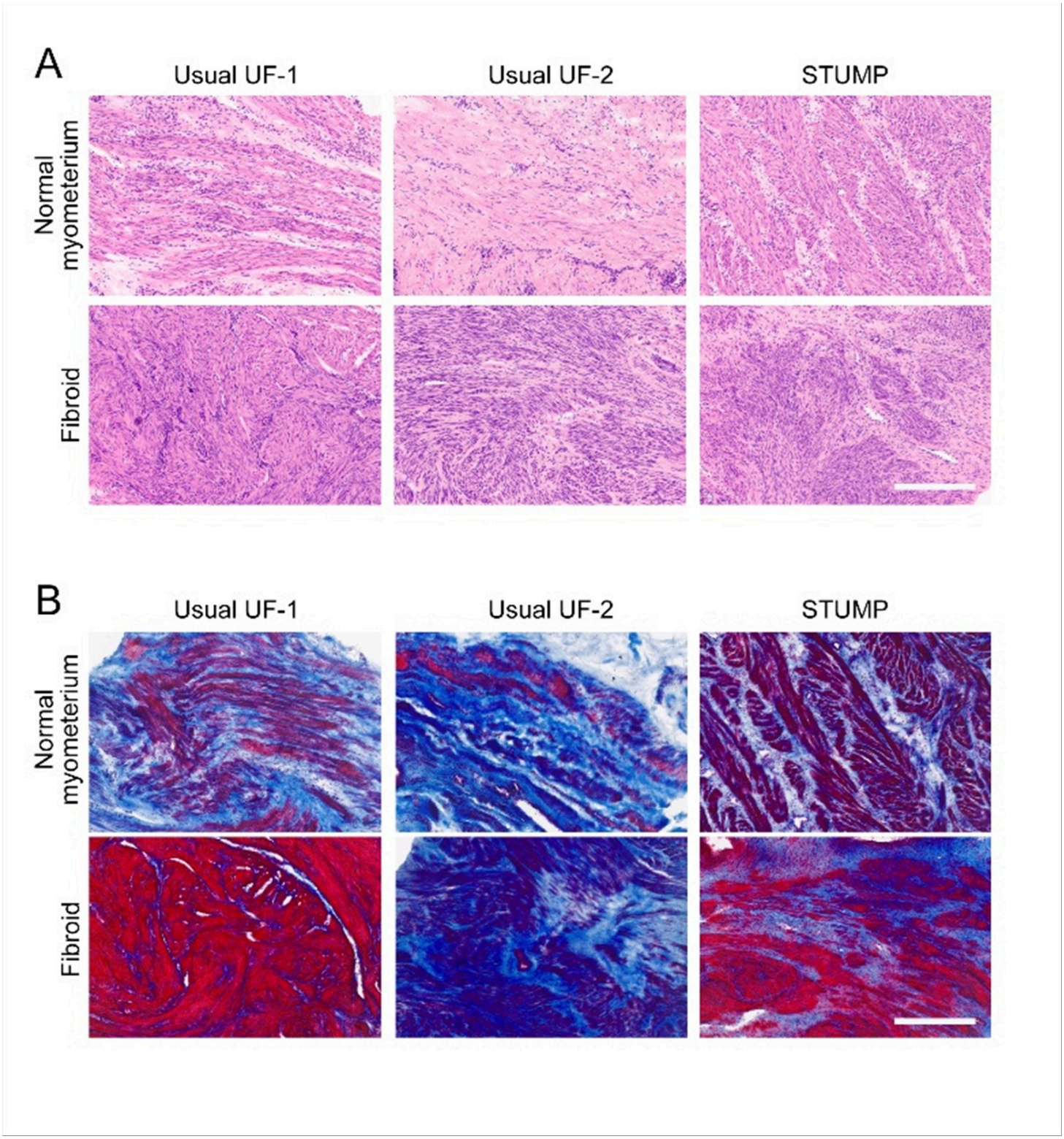


Figure 1

Histological characterization of normal myometrium and fibroid tissues. (A) Hematoxylin and eosin (H&E) staining of paired normal myometrium and UL tissues obtained from three independent patients used for primary culture including two cases of usual uterine fibroid (Usual UF-1, -2) and one case of smooth muscle tumor of uncertain malignant potential (STUMP). Representative images demonstrate the typical histoarchitecture of each tissue type. (B) Masson's trichrome staining of paired normal myometrium and UL tissues from the same patients, illustrating smooth muscle bundles and extracellular matrix organization. Scale bar: 300 mm

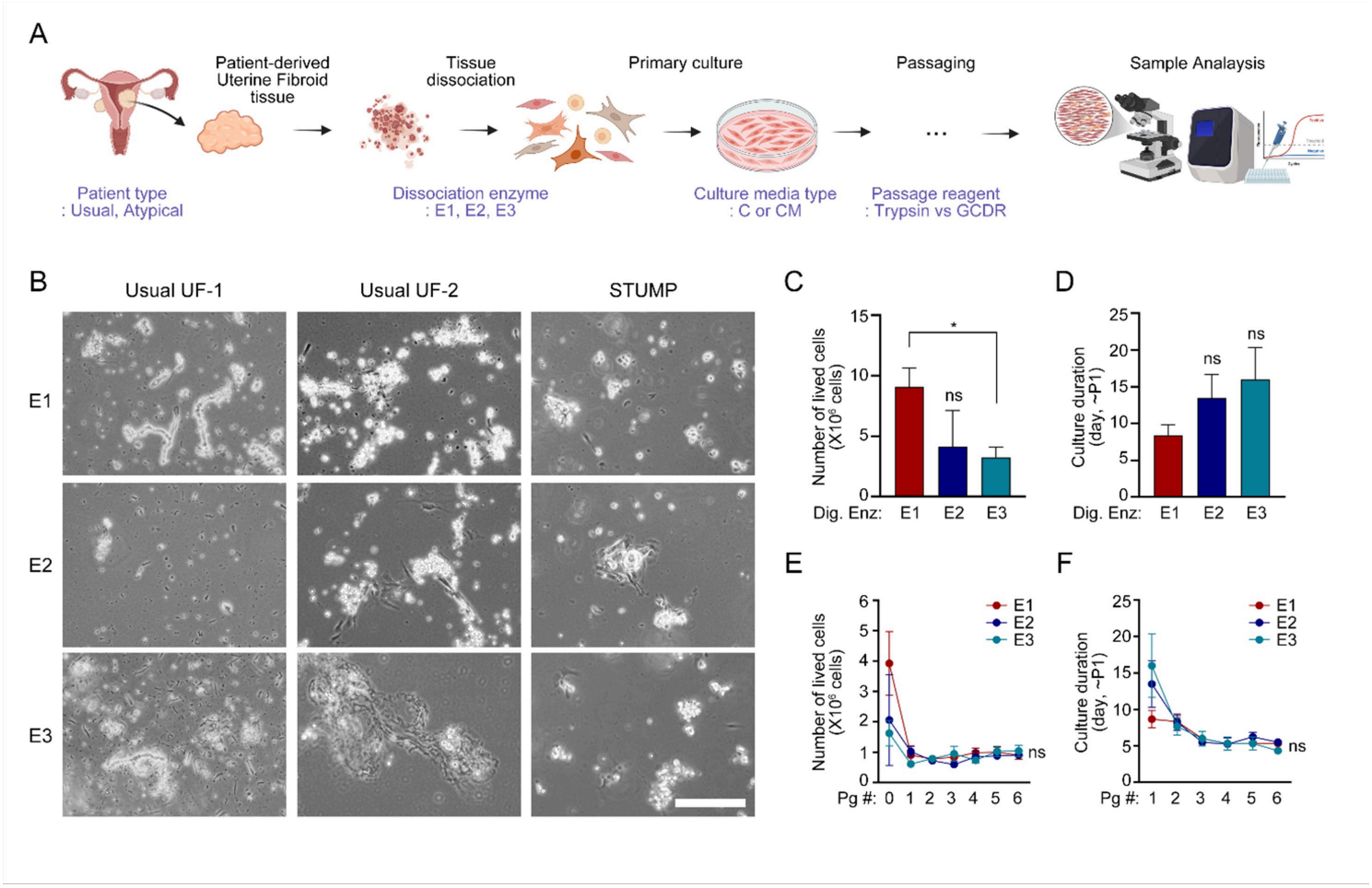


Figure 2

Effects of enzymatic dissociation conditions on primary UL cell yield and early culture dynamics. (A) Schematic overview of the experimental workflow for primary UL cell isolation, culture establishment, and longitudinal evaluation across serial passages. (B) Representative phase-contrast images of primary UL cells immediately after enzymatic dissociation using three different enzyme conditions (E1, E2, and E3). (C) Initial cell yield obtained at passage 0 (P0) following tissue dissociation with each enzyme condition. (D) Culture duration required to reach the detachment threshold for the first passage (P1) under each enzymatic dissociation condition. (E) Longitudinal cell yields from P0 to P6 under each enzyme condition. (F) Culture duration across serial passages (P1–P6) under each enzyme condition. Data are presented as mean ± SEM and *P < 0.05 was considered statistically significant. Scale bars: 0.5 mm.

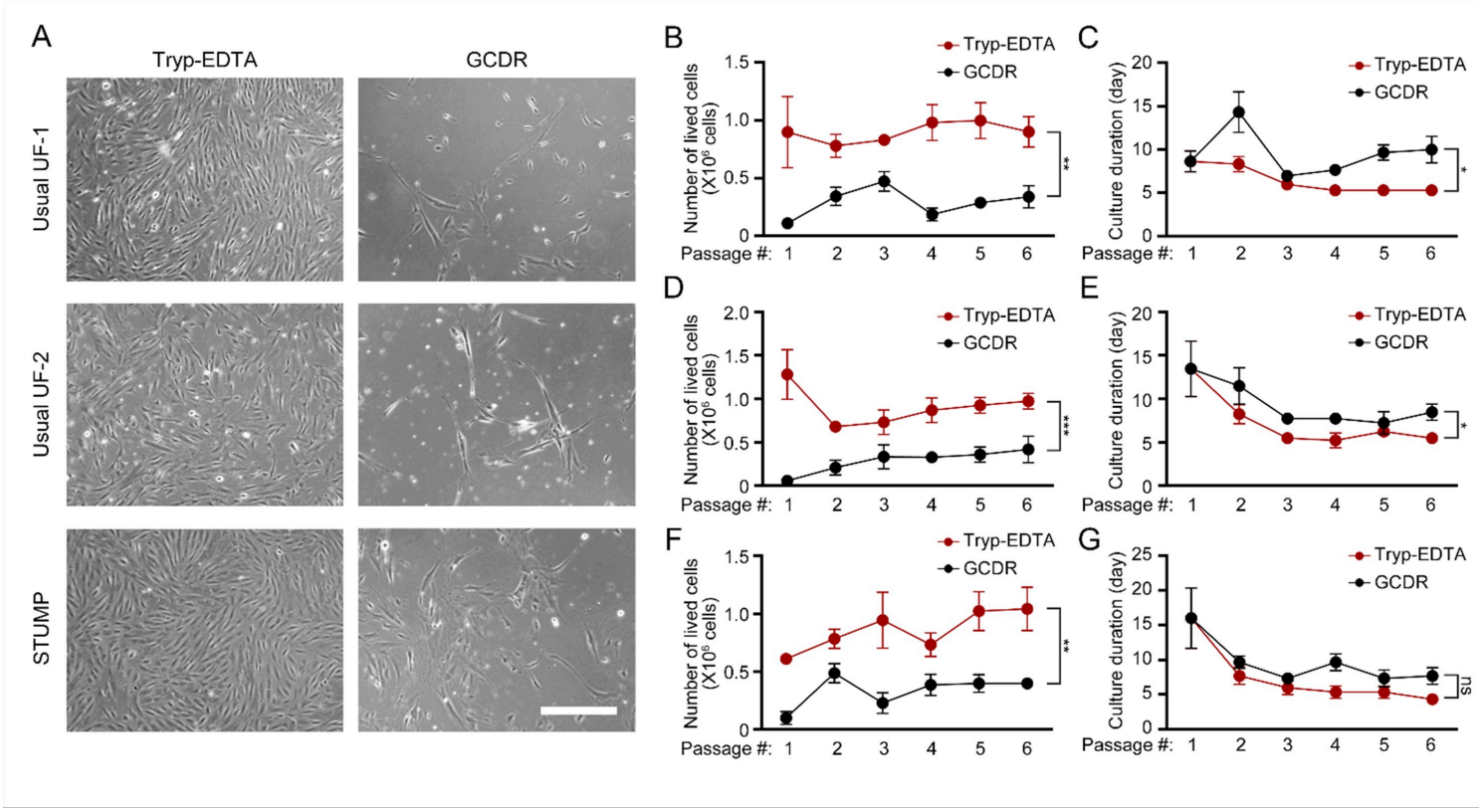


Figure 3

Differential effects of passaging methods on leiomyoma cell growth and culture duration. (A) Representative phase-contrast images of cultures established under E1 dissociation condition at passage 5 (P5; day 5) following serial passaging with trypsin-EDTA and GCDR, derived from usual uterine fibroid (Usual UF-1, -2) and STUMP samples. (B-C) Analyses under E1 enzymatic dissociation condition. (B) Cell yield obtained at each passage under the two detachment conditions. Trypsin-EDTA-treated cultures (red circles) and GCDR-treated cultures (black circles) are shown. Cell numbers at each indicated passage represent the total cells harvested at the preceding passage (e.g., P1 indicates cells collected at the end of P0 prior to passaging) (C) Culture duration required to reach the detachment threshold across serial passages. The indicated passage number corresponds to the time required to reach that passage (e.g., P1 represents the duration from initial seeding to the first passage). (D-G) Corresponding analyses for E2 (D, E) and E3 (F, G). Data are shown as mean ± SEM from three independent patients-derived cultures (n=3~4). *P < 0.05, **P < 0.01 and ***P < 0.001 were considered statistically significant. ns, non-significant. Scale bars: 0.5 mm.

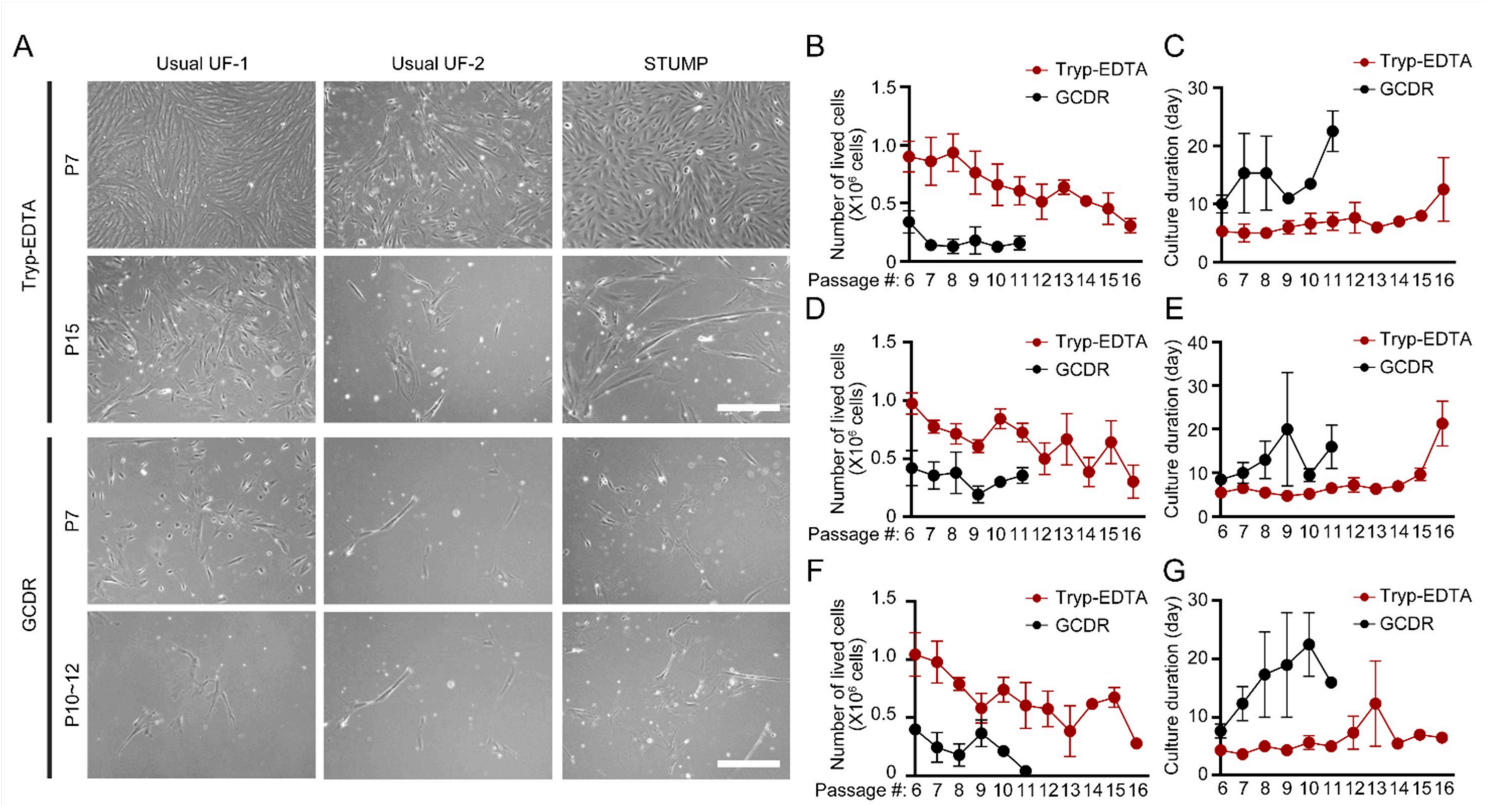


Figure 4

Non-enzymatic passaging accelerates loss of expansion capacity during long-term culture of primary UL cells. (A) Representative phase-contrast images of cultures derived from three independent patient samples (Usual UF-1, UF-2, and STUMP) under the E1 dissociation condition. Trypsin-EDTA–treated cultures are shown at passage 7 (P7) and passage 15 (P15), whereas GCDR-treated cultures are shown at P7 and earlier terminal passages (P10–12), reflecting limited long-term expansion. (B–C) Quantification of (B) cell yield and (C) culture duration across serial passages under the E1 dissociation condition. (D–E) Corresponding analyses under the E2 dissociation condition. (F–G) Corresponding analyses under the E3 dissociation condition. The passage number on the x-axis indicates the subsequent passage; cell yield represents cells harvested at the preceding passage, and culture duration indicates the time required to reach the indicated passage. Data are presented as mean ± SEM from independent patient-derived cultures (n = 3–4). Scale bars: 0.5 mm.

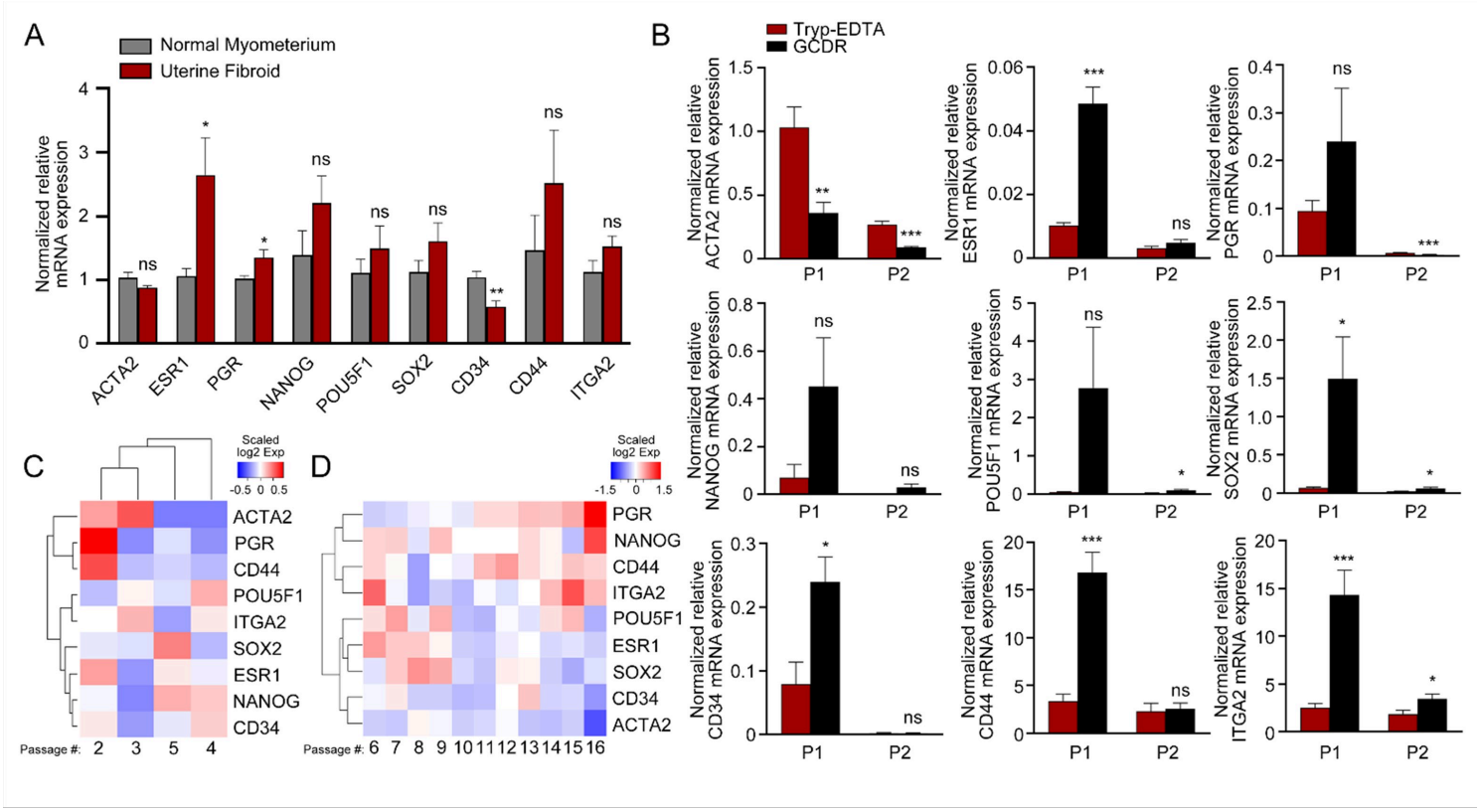


Figure 5

Tissue-to-culture transition and passage-dependent gene expression changes in primary UL cells. (A) Quantitative PCR (qPCR) analysis comparing gene expression levels between normal myometrium and uterine fibroid tissues. (B) qPCR analysis of UL-associated genes in primary cultures established under the E1 dissociation condition using either Trypsin-EDTA or GCDR at passages 1 (P1) and 2 (P2). Expression levels are shown relative to uterine fibroid tissue. Genes associated with smooth muscle identity, hormone responsiveness, stemness, and cell surface markers were analyzed. (C) Heatmap showing gene expression dynamics from P2 to P5 under the E1 Trypsin-EDTA condition. Expression values were normalized to the mean expression level of each gene across the indicated passages and scaled as z-scores to reflect relative variation. (D) Heatmap showing extended gene expression changes from P6 to P16 under the same culture condition, processed using the same normalization and scaling approach. Gene expression levels were determined by qPCR, normalized to the internal control gene (GAPDH), and expressed relative to uterine fibroid tissue. Data represent independent cultures derived from three patients (n = 3). *P < 0.05, **P < 0.01 and ***P < 0.001 were considered statistically significant. ns, non-significant.

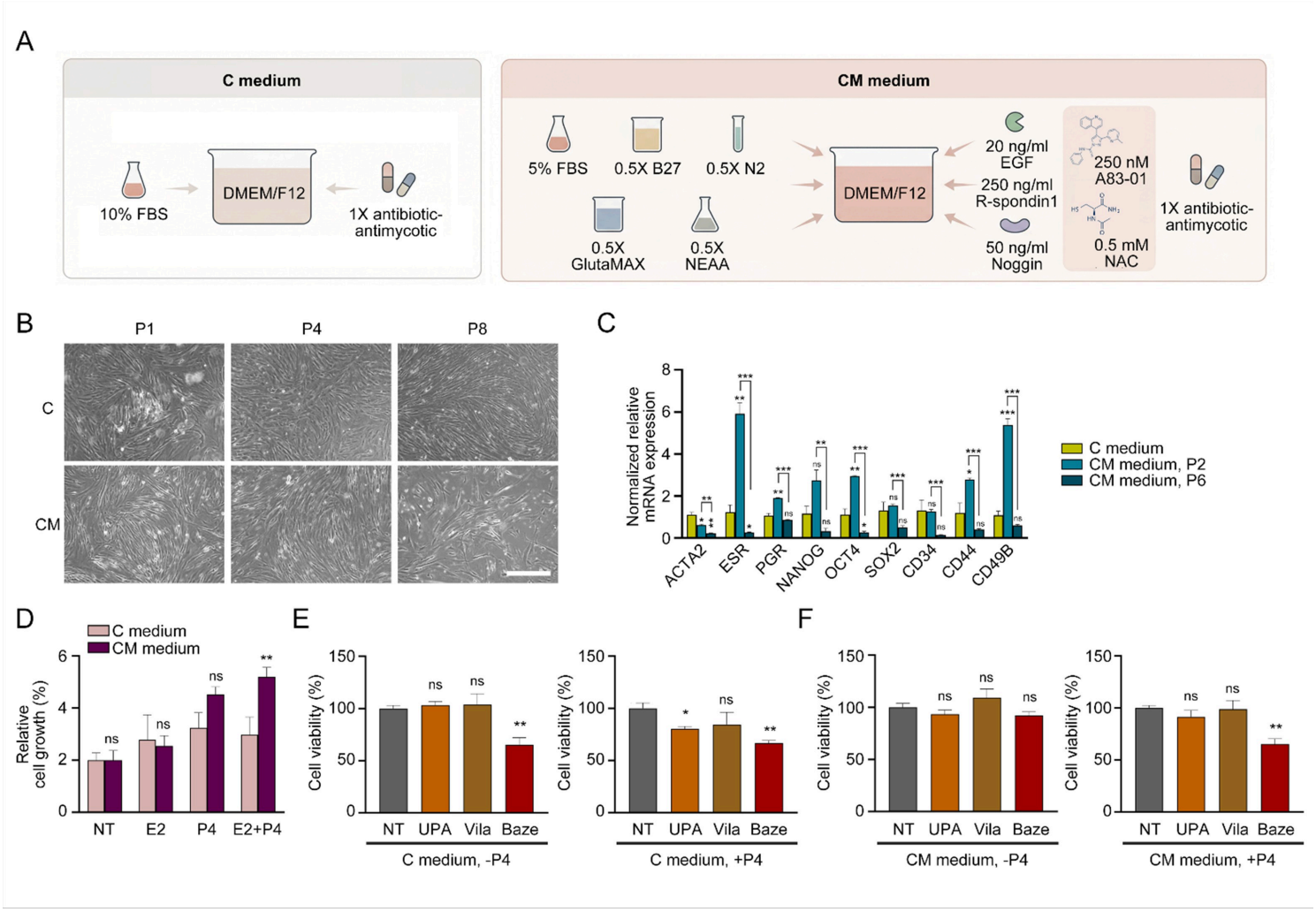


Figure 6

Optimized culture conditions transiently enhance cell expansion, gene expression, and hormone-dependent responses in primary UL cells. (A) Schematic representation of the composition of conventional serum-containing complete medium (C medium) and the optimized culture medium (CM medium) used for primary UL cell culture. (B) Representative phase-contrast images of UL cells cultured in C or CM medium at passages 1 (P1, Day 9), 4 (P4, Day 5), and 8 (P8, Day 8). (C) Relative expression levels of nine selected genes measured by qPCR in cells cultured in C medium, CM at passage 2 (CM-P2), and CM at passage 6 (CM-P6). (D) Cell viability of UL cells cultured in C or CM medium following hormone treatment. Cells were treated with vehicle control (NT), estradiol (E2), progesterone (P4), or combined E2+P4. (E-F) Effects of selective progesterone receptor modulators (SPRMs) on cell viability under different hormonal and culture conditions. (E) Cells cultured in C medium and (F) cells cultured in CM medium were treated with SPRMs in the absence (-P4) or presence (+P4) of progesterone. Cell viability was measured following treatment. Asterisks indicate statistically significant differences compared with the NT control within each condition. Statistical significance was determined using an unpaired Student's t-test. Data are presented as mean ± SEM. *P < 0.05, **P < 0.01 and ***P < 0.001 were considered statistically significant. ns, non-significant. Abbreviations: Baze, bazedoxifene; EGF, epidermal growth factor; FBS, fetal bovine serum; NAC, N-acetylcysteine; NEAA, non-essential amino acids; UPA, ulipristal acetate; Vila, vilaprisan. Scale bars: 0.5 mm.

Supplementary Files

This is a list of supplementary files associated with this preprint. Click to download.

- SupplementaryTables.docx

- SupFig12.tif
- SupFig22.tif
- SupplementaryFiguresandlegends.docx